Cross-linked Porous Gelatin Microparticles with Tunable Shape, Size, and Porosity

Cross-linked porous gelatin microparticles with tunable shape, size and porosity

Rita Gelli[a,†], Giulia Mugnaini[a,†], Tessa Bolognesi[a], Massimo Bonini[a,*]

a. CSGI & Department of Chemistry "Ugo Schiff", via della Lastruccia 3, 50019 Sesto Fiorentino (FI), ITALY
† These authors contributed equally to this publication

***Corresponding author**:
mail: massimo.bonini@unifi.it
phone: +39 055 457 3014

Abstract

Gelatin particles are relevant to many applications in the biomedical field due to their excellent biocompatibility and versatility. When prepared by double emulsion methods, porous microparticles with different architectures can be obtained. Controlling the shape, size, porosity, swelling, and stability against dissolution is fundamental toward their application under physiological conditions. We prepared porous gelatin microparticles from oil-in-water-in-oil emulsions, modifying the gelatin/surfactant ratio and the stirring speed. The effect on structural properties, including surface and inner porosities, was thoroughly assessed by multiple microscopy techniques (optical, electron, and confocal Raman). Selected samples were cross-linked with glutaraldehyde or glyceraldehyde, and their swelling properties and stability against dissolution were evaluated, while the influence of the cross-linking at the nanoscale was studied by scattering of X-rays. Depending on the preparation protocol, we obtained particles with different shapes (irregular or spherical), radii within ~40 to 90 μm, and porosities up to 10 μm. The crosslinking extends the stability in water from a few minutes up to several days while the swelling ability and the mesh size at the nanoscale of the gelatin network are preserved. The analysis of the experimental results as a function of the preparation parameters demonstrates that microparticles with tunable features can be designed.

Keywords

Gelatin; biopolymer; microparticles; porous; emulsions; double emulsions; cross-linking; glutaraldehyde; glyceraldehyde; swelling.

Abbreviations

GLU: glutaraldehyde; GAL: glyceraldehyde; FE-SEM: Field Emission Scanning Electron Microscopy; OM: Optical Microscopy; FT-IR: Fourier Transform-Infrared Spectroscopy; CCD: Charge-coupled device; SAXS: Small angle X-rays scattering; *q*: scattering vector; SD: standard deviation; O/W: oil-in-water; W/O: water-in-oil; O/W/O: oil-in-water-in-oil.

1. Introduction

Gelatin is a biopolymer obtained from the hydrolysis of collagen, which is the main protein constituting mammalians' connective tissues. Collagen is insoluble in water, but thermal and chemical (acidic or alkaline) treatments denaturate its triple-helix structure, resulting in a water-soluble protein, *i.e.* gelatin (Harris et al., 2003). Above ~40 °C, gelatin is dissolved in water as the polymeric chains behave as random coils while the collagen-like triple-helices partially reform upon cooling, leading to the formation of a physical gel (JL Gornall, 2008). Gelatin is highly biocompatible, versatile, inexpensive and easily available (Campiglio et al., 2019), and its use is well-established in several fields, namely food, confectionery, pharmaceutical, medical and cosmetic (Haug & Draget, 2011). Gelatin's applications in the biomedical field are widespread (Bello et al., 2020; Su & Wang, 2015), given the presence in its structure of cell-recognition motifs, such as the amino acidic sequence Arg-Gly-Asp (RGD), which improve the final biological performances of the material (Santoro et al., 2014); however, due to its solubility close to physiological temperature, it is often necessary to enhance gelatin's resistance to dissolution by means of physical, chemical or enzymatic cross-linking strategies (Campiglio et al., 2019). Among chemical cross-linkers, aldehydes such as formaldehyde (Moll et al., 1974) and especially glutaraldehyde (Bigi et al., 2001; M. C. Chang & Tanaka, 2002) were commonly used in the past, being very effective in reacting mainly with amines from lysine residues in gelatin chains; however, their use raised some concerns regarding the final toxicity of the cross-linked material due to unreacted cross-linker molecules (Gao et al., 2017; Han et al., 2003). More biocompatible alternatives include EDC/NHS (1-ethyl-3-(3-dimethylaminopropyl)carbodiimide/*N*-hydroxysuccinimide) (J.-Y. Chang et al., 2007; Kuijpers et al., 2000; Zhang et al., 2009), genipin (Bigi et al., 2002; Liang et al., 2004; Lien et al., 2008), glyceraldehyde (Sisson et al., 2009; Vandelli et al., 2001) and diglycidyl ethers (J. R. Dias et al., 2017; Nagura et al., 2002; Vargas et al., 2008).

The versatility of gelatin makes it possible to prepare materials with different characteristics, such as fibers (Choktaweesap et al., 2007; Ratanavaraporn et al., 2010), films (Ahammed et al., 2020; Rao, 2007), scaffolds (Gelli et al., 2018; Wu et al., 2010), composite hydrogels (Tatini et al., 2015), nanoparticles (Elzoghby, 2013) and microparticles (Esposito et al., 1996). The latter category is

particularly relevant in several fields including drug delivery (Foox & Zilberman, 2015), tissue engineering (Sulaiman et al., 2020), and for the development of microscaffolds for cells culture, in which cells attach and spread on solid microspheres and gradually grow and propagate on the surface of the microspheres or in the pores of the macroporous structure (Ma & Su, 2013). Gelatin microparticles can be prepared by means of several techniques, such as spray drying, precipitation, solvent evaporation, and emulsification. The latter technique involves the dissolution of gelatin in water, with the subsequent addition in hydrophobic media (typically olive oil) under stirring in order to form water-in-oil (W/O) emulsions (Sulaiman et al., 2020). Surfactants are often used to improve the final characteristics of the microparticles, such as stability, uniformity and monodispersity (Esposito et al., 1996; Kim et al., 2009; Xia et al., 2019; Yuan et al., 2019).

The emulsification technique allows also for the preparation of porous gelatin microparticles following a double emulsion method (Garti & Bisperink, 1998). This approach was first proposed by Nilsson *et al.* (Nilsson et al., 1986), who prepared porous gelatin microparticles with an oil-in-water-in-oil (O/W/O) emulsion where the oil phase is toluene, taking advantage of different surfactants to stabilize both the O/W and W/O interphases. A similar approach was used by Tao *et al*., who obtained two types of gelatin porous particles (pore size < 1 μm and 5-10 μm) by varying the stirring speed and used them to cultivate hepatocytes, demonstrating that pore size plays an important role in the adhesion and metabolic function of cells in culture (Tao et al., 2003). Porous gelatin particles can also be prepared with different strategies, such as air-in-water-in-oil emulsions to obtain gelatin sponge millispheres (Yamashita et al., 2009), W/O emulsions where NaCl generates the porosities (Lan et al., 2017), freeze-drying methods (Li et al., 2020) or casting strategies with $CaCO_3$ as template (Wang et al., 2012). Gelatin porous microparticles are typically cross-linked to make them stable against dissolution at physiological temperature, either by means of glutaraldehyde (Li et al., 2020; Nilsson et al., 1986; Tao et al., 2003) or glyceraldehyde (Imparato et al., 2013). This process is essential for applications in the biomedical field, where the use of these materials provides several advantages: with respect to other biocompatible polymers, gelatin promotes cells' attachment and growth due to the presence of cells-interacting motifs, and it is even used to coat the surface of microparticles made with non-bioactive matrices (Ma & Su, 2013) or in combination with other polymers like chitosan (Karimian S.A. et al., 2016), alginate (Devi & Kakati, 2013) and starch (Phromsopha & Baimark, 2014). In addition, when compared to solid microparticles, the porous counterparts provide an environment closer to that found *in vivo* (Ma & Su, 2013) and the larger surface provided by both the external surface and the internal porosities results in improved cells' attachment and growth (Nikolai & Hu, 1992). Porosity is also crucial in the field of drug delivery, allowing for an efficient drug

entrapment and for a release kinetic controlled by the size, shape and interconnection of the porous structure (Ghosh Dastidar et al., 2018; Lengyel et al., 2019).

Despite gelatin porous microparticles being commercially available (Bancel & Hu, 1996; Huss et al., 2007, 2010; Lönnqvist et al., 2015; Ng et al., 1996; Nikolai & Hu, 1992; Rodrigues, 2013; Shiragami et al., 1993), in general the non-customizability of the microcarrier's properties hampers their application (A. D. Dias et al., 2017). Therefore, the control of shape, size and porosity of these materials would be crucial to further boost the application of gelatin-based microparticles. Double emulsion methods may offer this possibility, as the modification of preparation protocol and processing parameters such as polymer concentration, surfactant concentrations and the stirring speed could in principle lead to the formation of different types of microparticles; nevertheless, to the best of our knowledge, the precise effect of the modification of various experimental conditions in double emulsion methods on the features of gelatin microparticles is unexplored in the literature.

In this work, we prepared porous gelatin-based microparticles by means of a double emulsion method by systematically varying the amount of surfactant and the stirring speed used in the preparation. The obtained microparticles were characterized in terms of morphology and porosity by means of different microscopy techniques (optical, electron and confocal Raman), and selected samples were then chemically cross-linked with glutaraldehyde and glyceraldehyde. The swelling and dissolution behavior of cross-linked samples was studied, while scattering techniques were used to analyze the structure at the nanoscale. The results were correlated with the preparation parameters, demonstrating the possibility of tuning the shape, the size, the porosity, the swelling and the dissolution of the samples, allowing for the design of microparticles with desired features.

2. Materials and methods

2.1 Materials

Gelatin from porcine skin (type A) was obtained from Fluka Analytical (Milan, Italy). Polyethylene glycol sorbitan monooleate (TWEEN 80) was purchased from Merck (Rome, Italy) and sorbitan trioleate (SPAN 85) was obtained from Bregaglio S.r.l. (Biassono, Italy). Toluene (purity ≥ 99.8 % GLC), acetone (purity ≥ 99.8 % GLC) and ethanol (absolute denatured ≥ 99.2 %v/v) were purchased from Carlo Erba (Milan, Italy). D,L-Glyceraldehyde (purity ≥ 90 % GC) and glutaraldehyde (50 %wt in H_2O) were obtained from Sigma-Aldrich (Milan, Italy). All the reagents were used without further purification.

2.2 Gelatin microparticles preparation

Gelatin microparticles were prepared following a double emulsion oil-in-water-in-oil (O/W/O) approach, as previously described (Imparato et al., 2013). In Step I, 0.8 g of gelatin were dissolved

in 10 mL of deionized water, and different amounts of TWEEN 80 were added (see Table 1). The solution was kept under stirring at 60 °C. 5 ml of a toluene solution containing SPAN 85 (3 % w/v) were added to the gelatin solution in order to obtain the primary oil-in-water (O/W) emulsion. In Step II, toluene (25 ml) was added to the primary emulsion and the stirring speed was increased, as reported in Table 1, leading to the formation of gelatin beads containing droplets of toluene. The mixture was cooled down to 10 °C, then 20 ml of cold ethanol were added to extract toluene. Gelatin porous microparticles were washed with cold acetone, filtered and dried at room temperature. The resulting microparticles were dimensionally selected with a sieve (Sieve, Endecotts Ltd, London SW19 3RB, England) with a cut-off of 425 μm. A schematic representation of the preparation process is reported in Figure 1.

Table 1. Experimental conditions and nomenclature of gelatin porous microparticles samples.

Sample	Gelatin†	TWEEN 80	SPAN 85‡	Toluene	Step I Stirring speed	Step II Stirring speed
T3_500	10 ml	0.3 g	5 mL	25 mL	300 rpm	500 rpm
T3_750	10 ml	0.3 g	5 mL	25 mL	300 rpm	750 rpm
T3_1000	10 ml	0.3 g	5 mL	25 mL	300 rpm	1000 rpm
T6_500	10 ml	0.6 g	5 mL	25 mL	300 rpm	500 rpm
T6_750	10 ml	0.6 g	5 mL	25 mL	300 rpm	750 rpm
T6_1000	10 ml	0.6 g	5 mL	25 mL	300 rpm	1000 rpm
T9_500	10 ml	0.9 g	5 mL	25 mL	300 rpm	500 rpm
T9_750	10 ml	0.9 g	5 mL	25 mL	300 rpm	750 rpm
T9_1000	10 ml	0.9 g	5 mL	25 mL	300 rpm	1000 rpm

† Solution of Gelatin in water (8% w/v)

‡ Solution of SPAN 85 in toluene (3% w/v)

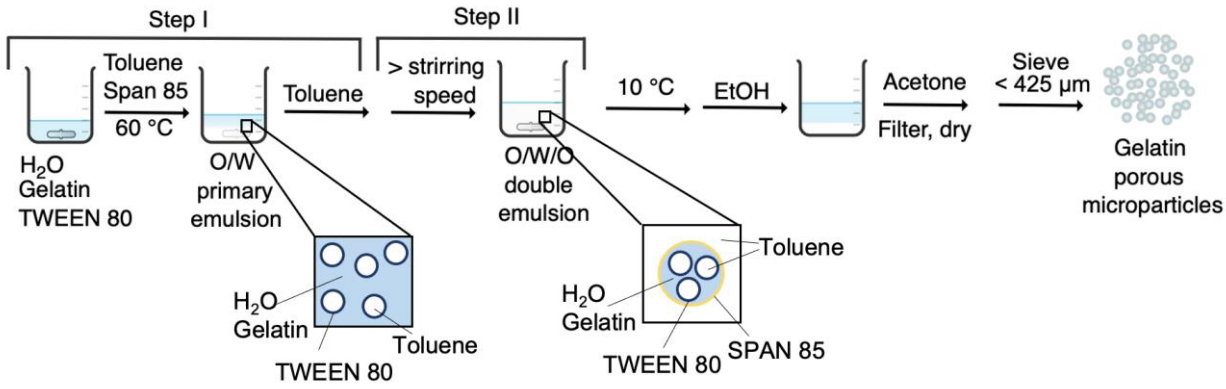

Figure 1. Schematic representation of the process for the preparation of gelatin porous microparticles.

2.3 Cross-linking

Samples of gelatin microparticles differing for TWEEN 80 concentration and stirring speed of Step II (T3_500, T6_500 and T9_1000) were chemically cross-linked using glutaraldehyde (GLU) and glyceraldehyde (GAL) to improve their stability against dissolution in aqueous environment at human body temperature. In particular, 30 mg of gelatin microparticles were dispersed in 6 ml of acetone containing 1.5 mg of GLU (3 µl of a GLU solution 50 % wt in H_2O); for GAL, 30 mg of gelatin microparticles were dispersed in 4 ml of acetone containing 300 µl of water and 1.5 mg of GAL. The dispersions were kept at 5 °C for 24 h, then the resulting microparticles were filtered, washed with acetone, dried at room temperature and sieved with a 425 µm-cut-off sieve (Sieve, Endecotts Ltd, London SW19 3RB, England).

2.4 Characterization techniques

2.4.1 Field Emission- Scanning Electron Microscopy (FE-SEM)

The morphology of the gelatin microparticles was investigated by means of FE-SEM microscopy, using a Zeiss ΣIGMA microscope. The dried microparticles were fixed on aluminum stubs by means of conductive tape. The micrographs were collected on pristine samples (no coating was performed to improve conductivity) with an accelerating voltage of 1.5 kV, working distance ~7 mm and using the secondary electrons detector.

2.4.2 Optical Microscopy (OM)

Gelatin microparticles were analyzed by means of optical microscopy, using a transmission bright-field Nikon Diaphot 300 equipped with a Nikon PSM-2120 lamp. The particles were observed with a 10X objective and the images were acquired by means of a CCD Nikon Digital Sight DS-U1. The collected micrographs were analyzed with the program ImageJ (Schneider et al., 2012) measuring

about 100 objects for each sample. The results were used to obtain the size distribution curves, which were fitted using a Gaussian function (Equation 1):

$$y = A \cdot exp\left[-\left(\frac{x - x_0}{\sqrt{2} \cdot \sigma}\right)^2\right] \quad \text{Equation 1}$$

where A is the amplitude, x_0 is the peak's position and σ is the standard deviation (SD).

2.4.3 Confocal Raman Microscopy

The internal structure of dry microparticles was investigated by acquiring 3D volume maps by means of confocal Raman microscopy, using an InVia^{TM} Renishaw microscope. Maps were collected using a 100X objective and a laser operating at 785 nm with a power of 50 %. For each sample, a volume of 24 µm x 16 µm x 20 µm (*xyz* directions, respectively) was scanned recording Raman spectra every 2 µm (on the *xy* plane and along the *z* axis). Spectra were corrected for cosmic rays, baseline and noise, and then used to obtain volume maps based on the signal-to-baseline intensity in the 1200 cm^{-1} to 1700 cm^{-1} region.

2.4.4 Small-Angle X-Rays Scattering (SAXS)

SAXS experiments were carried out with a HECUS SWAX camera (Kratky) equipped with a position-sensitive detector (OED 50 M) containing 1024 channels of width 54 µm. Cu Kα radiation of wavelength 1.542 Å was provided by a Seifert ID-3003 X-rays generator (sealed-tube type), operating at a maximum power of 27 W (30 kV and 0.9 mA). All the scattering curves were recorded in the *q*-range between 0.012 and 0.55 $Å^{-1}$. Hydrated microparticles were sealed in a cell between two Kapton windows. Scattering curves were corrected for the water and Kapton contributions. The data were analyzed with SasView software (http://www.sasview.org/).

2.4.5 Swelling

The water absorption properties of gelatin microparticles were investigated by means of optical microscopy (see 2.4.2). Dry microparticles were placed between two staggered microscope slides and then a drop of water was led by capillarity in between the glass slides. Images of single microparticles were acquired before and 10 minutes after water addition. The experiments were conducted at room temperature and at 37 °C, by using a Peltier heating/cooling microscope stage. The collected images were used to obtain the diameter of dry and swelled microparticles using the software ACT-2U (Nikon Corporation). All the experiments were made in triplicate. The swelling ratio was calculated according to Equation 2:

$$Swelling\ ratio = \frac{diameter_{swelled}}{diameter_{dry}} \quad \text{Equation 2}$$

2.4.6 Dissolution

The dissolution of gelatin microparticles at 37 ˚C in water was assessed by means of optical microscopy (see 2.4.2). Dry microparticles were placed in between two staggered microscope slides placed on top of a Peltier sample stage at 37 ˚C, and then a drop of water was led inside by capillarity. The images of the microparticles were taken during the next two hours. In parallel, dry microparticles were added to water (1 mg/mL) at 37 ˚C and visually inspected until they were no longer visible.

3. Results and discussion

The morphology of the microparticles prepared as described in detail in the section 2.2 was analyzed by means of FE-SEM: while at low magnifications we can observe the shape and the size of the particles, at high magnifications information about their porosity are obtained. The micrographs reported in Figure 2 show the overall morphology of the particles, which is markedly different depending on the preparation protocol. Spherical microparticles are obtained at high TWEEN 80 content, as samples prepared with a gelatin/TWEEN 80 ratio of 8/3 display irregular shapes, especially when low stirring speeds are used. When high TWEEN 80 content and fast stirring are combined (*i.e.* samples T9_750 and T9_1000), very regular and spherical particles are obtained.

The size distribution curves were obtained by imaging the microparticles by optical microscopy (see Figure S1). The resulting distributions were fitted with a Gaussian function and the mean radii and standard deviations obtained for each sample are given in Table 2. The plot of the particles' radius as a function of the stirring speed used in the preparation, shown in Figure 3, clearly highlights the linear relationship between the two parameters: in fact, increasing the stirring speed in the second step of the preparation from 500 to 1000 rpm allows one to reduce particles' size of about 1/3. An increase in the stirring speed also results in less polydisperse distributions, as it appears from the standard deviations reported in Table 2.

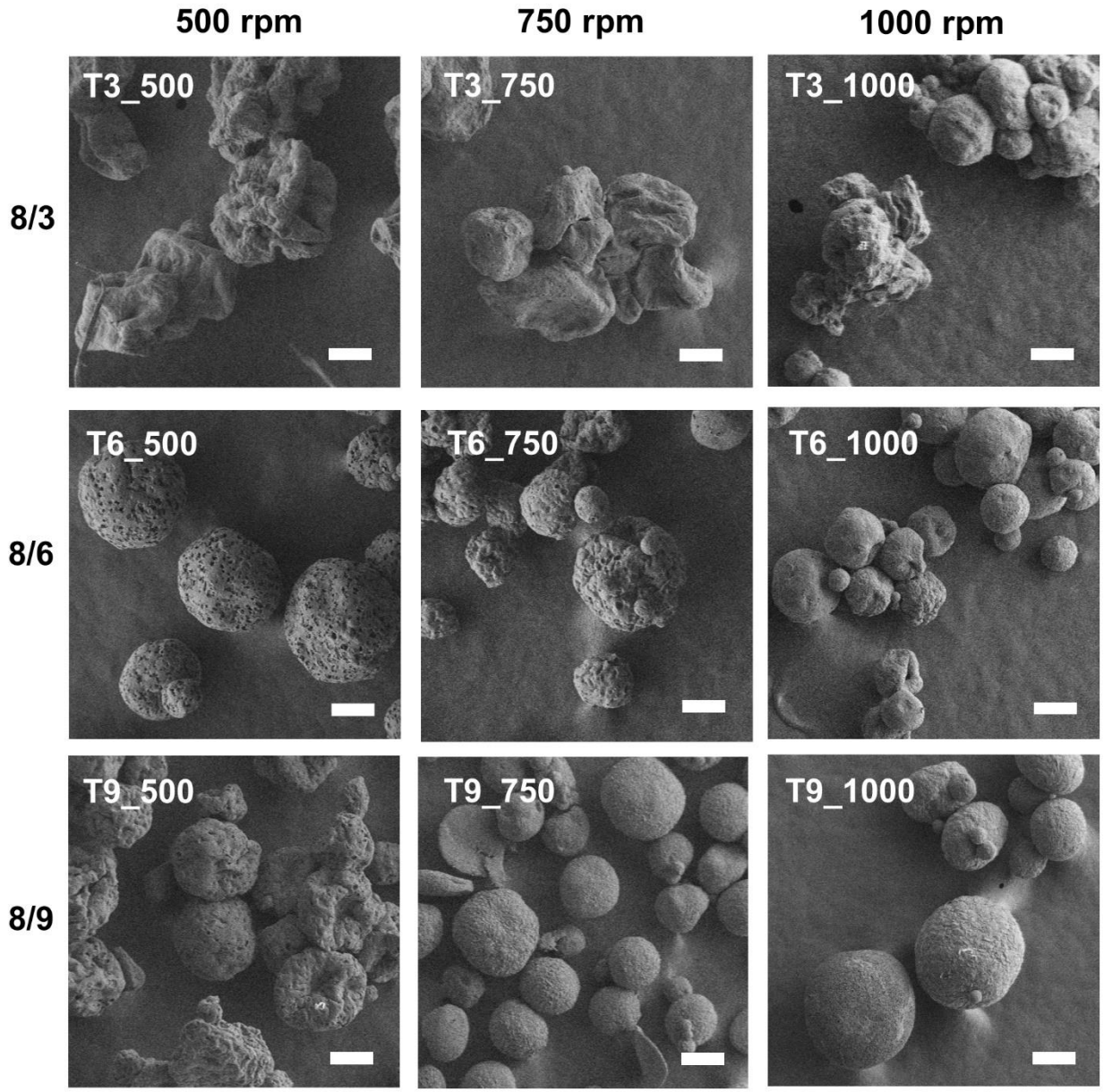

Figure 2. FE-SEM micrographs at 250X of the prepared gelatin microparticles. 500 (first column), 750 (second column) and 1000 rpm (third column) indicate the stirring speed used in the Step II of the preparation, whereas 8/3 (first row), 8/6 (second row) and 8/9 (third row) indicate the gelatin/TWEEN 80 ratio. The scale bar is 100 µm.

Table 2. Morphological parameters of the prepared gelatin microparticles.

Sample	Radius (µm)[†]	SD (µm)[†]	Pore range (µm)[‡]
T3_500	88.4 ± 2.2	26.4 ± 2.3	1 - 10
T3_750	71.2 ± 2.4	19.4 ± 2.4	0.1 - 5
T3_1000	55.4 ± 1.7	15.8 ± 1.7	0.1 - 1

T6_500	60.8 ± 0.6	15.8 ± 0.6	1 - 10
T6_750	52.1 ± 1.5	15.6 ± 1.6	0.1 - 10
T6_1000	40.5 ± 1.2	11.7 ± 1.2	0.1 - 5
T9_500	71.2 ± 1.3	22.7 ± 1.3	0.1 - 10
T9_750	53.9 ± 1.7	20.7 ± 1.8	0.1 - 1
T9_1000	50.1 ± 2.2	19.7 ± 2.1	0.1 - 1

† Resulting from the Gaussian fits of the size distribution curves obtained from OM images. The associated errors are obtained from the fitting.

‡ Estimated from FE-SEM micrographs.

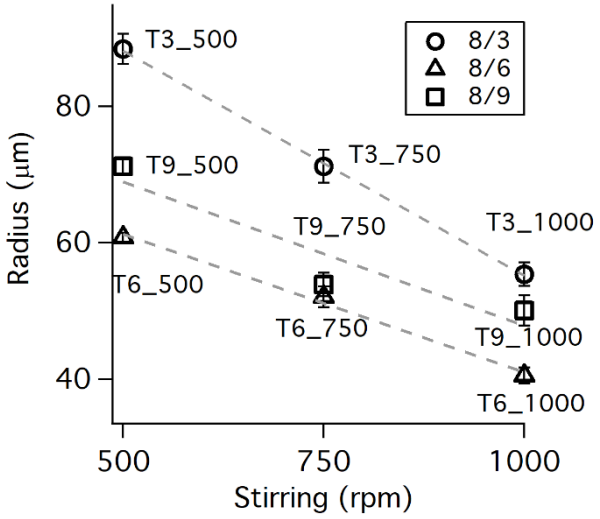

Figure 3. Plot of the particle's radius as a function of the stirring speed used in the second step of the preparation. 8/3, 8/6 and 8/9 indicate the gelatin/TWEEN 80 ratio. The error bars associated to the markers result from the fitting (see Table 2).

The porosities of the microparticles were analyzed by observing high magnification FE-SEM micrographs (see Figure 4). All samples show interconnected macroporosities, ranging from hundreds of nm to tens of µm (see Table 2). The size and the shape of the pores are strongly affected by the preparation protocol: in fact, larger pores are obtained at low stirring speeds and low surfactant concentration, whereas fast stirring and high TWEEN 80 content both lead to smaller porosities. It is important to point out that non-spherical samples, such as T3_500 and T3_750, are also endowed with some indentations and interstices on the surface which are tens of µm-sized and that provide the particles with an additional level of porosity (see Figure 2).

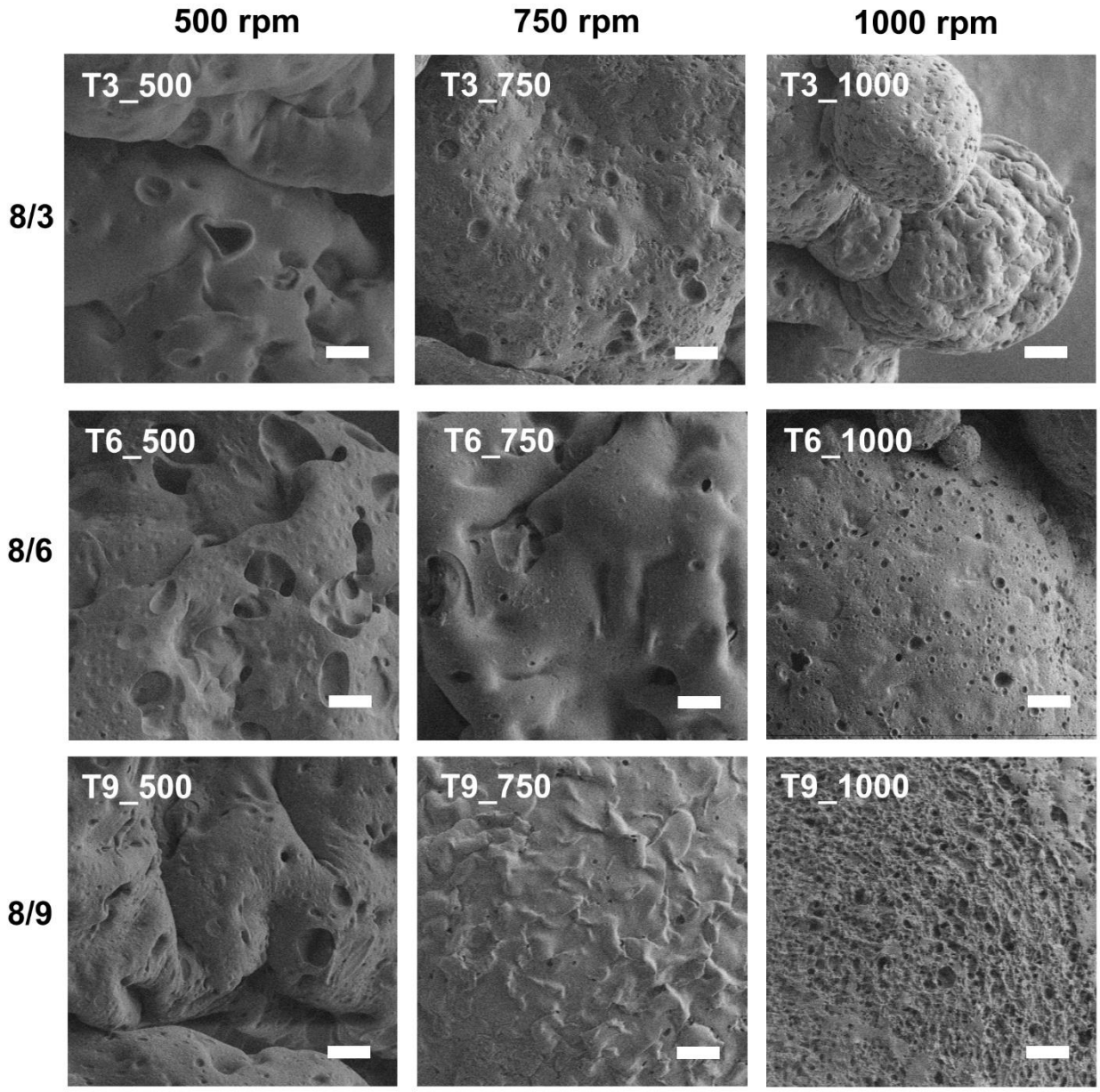

Figure 4. FE-SEM micrographs at 2500X of the prepared gelatin microparticles. 500 (first column), 750 (second column) and 1000 rpm (third column) indicate the stirring speed used in the Step II of preparation, whereas 8/3 (first row), 8/6 (second row) and 8/9 (third row) indicate the gelatin/TWEEN 80 ratio. The scale bar is 10 μm.

Together with the tunability of shape, size and surface porosity, a crucial aspect towards the utilization of these microparticles in actual applications is the knowledge of the inner structure: in fact, one could wonder if the surface pores extend towards the inner part of the particles and if those pores are interconnected. To this purpose, the internal structure of the microparticles was investigated by means of confocal Raman microscopy, collecting 3D maps of dry microparticles. Samples T3_500, T6_500 and T9_1000 were selected as representative of the different morphologies and porosities obtained

with different preparation protocols. The 3D maps were obtained by collecting Raman spectra of the samples (see Figure S2 in the Supplementary Material for representative spectra of each sample) from a volume of 24 µm x 16 µm x 20 µm (*xyz* directions, respectively), with a spatial resolution of 2 µm (*i.e.*, 1287 spectra per each sample). Figure 5 reports representative *xyz* slices per each sample, where the intensity of the color accounts for the signal-to-baseline value between 1200 and 1700 cm^{-1}, which reflects gelatin's amount. Dark areas in the maps are therefore indicative of voids and pores (3D reconstructions videos for T3_500, T6_500 and T9_1000 are provided as Video 1, Video 2 and Video 3, respectively). All the samples display the presence of interconnected pores inside the particles, demonstrating that the porosity observed in FE-SEM micrographs on the surface of the particles is representative of the entire structure, which is of outmost importance in view of the application of these materials as, for instance, microscaffolds for cell growth and drug delivery vehicles.

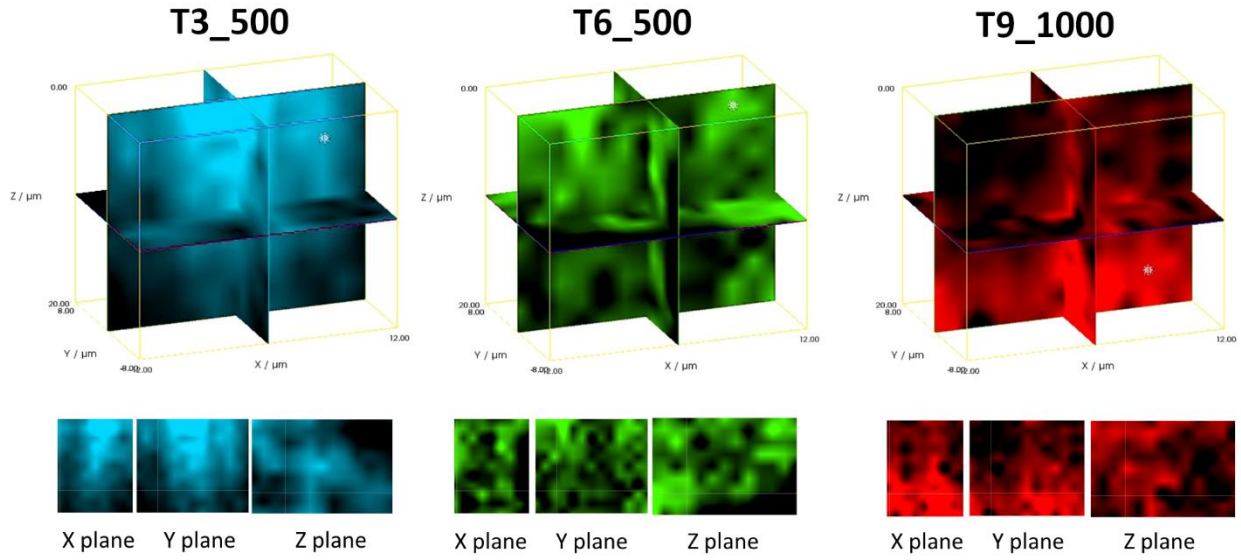

Figure 5. Confocal Raman volume maps of samples T3_500, T6_500 and T9_1000 (*x*, *y* and *z* slices). The maps volume is 24x16x20 μm^3 (*xyz*, respectively). The color intensity accounts for the intensity of gelatin signals in the corresponding Raman spectra, *i.e.* darker areas correspond to void areas.

One of the main limitations in the use of gelatin-based systems, especially in biomedical and food applications, is its poor stability against dissolution in water at 37 °C: in fact, the use of gelatin in those applications often requires that the system does not dissolve (or, at least, not too rapidly) and/or that its architecture remain almost unaffected for hours or days. To overcome this limitation, we investigated the effect of two bifunctional chemical cross-linkers, namely glutaraldehyde (GLU) and glyceraldehyde (GAL). Glutaraldehyde was chosen as it is one of the most frequently used chemical cross-linkers for gelatin, even though recent concerns have been raised about potential toxicity issues

(Gao et al., 2017; Han et al., 2003). As an alternative, we also selected glyceraldehyde which has been suggested as a biocompatible cross-linking agent (Vandelli et al., 2001). The reaction for both cross-linking reagents mainly occurs between the aldehydic terminal units of GLU and GAL and the ε-amine groups of lysine or hydroxylysine residues through an aldol condensation reaction, resulting in a Schiff base intermediate (Nguyen et al., 2015). The same samples selected as representative for the Raman investigation were reacted with both cross-linkers (see section 2.2). The morphology of the cross-linked microparticles was examined by means of FE-SEM and the results, reported in Figure S3, show that neither shape, size nor porosity are affected by the treatment. To assess if the cross-linking induces a change in the structure of the microparticles at the nanoscale, hydrated samples (*i.e.*, swelled microparticles) were investigated by means of Small Angle Scattering of X-rays. The experimental data of T3_500, T6_500 and T9_1000, pristine and cross-linked with GLU and GAL, are reported in Figure 6, together with the corresponding fittings. Experimental data were analyzed according to a model previously used for the fitting of gelatin hydrogels (Pezron et al., 1991; Vesperinas et al., 2006). The scattered intensity includes two contributions:

$$I(q) = I_{Lorentz}(q) + I_{excess}(q) + bkg \qquad \text{Equation 3}$$

The *Lorentzian* contribution accounts for the formation of transient networks in the matrix, while the *excess* term, derived from the Debye-Bueche theory, accounts for the deviation at low q values due to the contribution to the scattering from inhomogeneities:

$$I_{Lorentz}(q) = \frac{I_{Lorentz}(0)}{1+q^2\xi^2} \qquad \text{Equation 4}$$

$$I_{excess}(q) = \frac{I_{excess}(0)}{(1+q^2a^2)^2} \qquad \text{Equation 5}$$

where ξ is the average mesh size of the transient networks formed by gelatin chains, a is the size of inhomogeneity domains and *bkg* is the incoherent background from the measurement. In our case, data were first analyzed by plotting the inverse scattered intensities, $1/I(q)$, as a function of q^2, since a linear dependence is expected from the *Lorentzian* contribution. The results (see Figure S4 in the Supplementary Material) show that a deviation from the linear behavior is observed only for few experimental points at the lower q values (*i.e.*, $q < 1.8 \cdot 10^{-2}$), suggesting that the *Lorentzian* contribution dominates the curve in the investigated q range and that inhomogeneity domains are too big to be accurately evaluated by our instrumental setup. SAXS curves were therefore fitted without any *excess* contribution and not considering the experimental points deviating from the q^2 dependence at low q. The results reported in Table 3 show that the average mesh size agrees with value reported in literature for gelatin hydrogels (Vesperinas et al., 2006). Furthermore, the cross-linking procedure does not hinder the ability of the hydrated gelatin chains to form transient networks at the nanoscale, as confirmed by ξ the values.

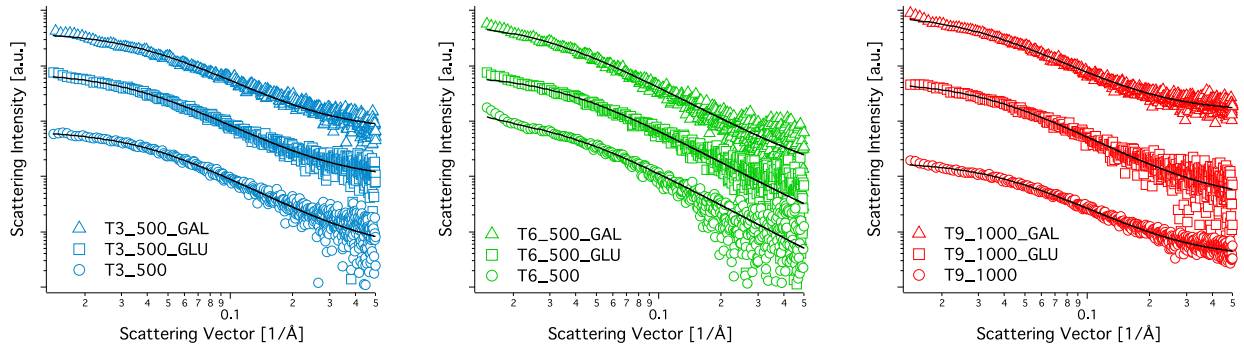

Figure 6. SAXS spectra (markers) together with the corresponding fitting (black lines). Curves were off-set for the clarity of presentation.

Table 3. Average mesh size of the transient network formed by gelatin chains and swelling ratios of gelatin microparticles.

Sample	ξ [Å]†	Swelling ratio‡
T3_500	26.1 ± 0.3	2.2 ± 0.2
T3_500_GLU	27.0 ± 0.3	3.4 ± 0.7
T3_500_GAL	26.9 ± 0.4	3.1 ± 0.6
T6_500	30.0 ± 0.4	3.6 ±0.8
T6_500_GLU	30.6 ± 0.4	2.6 ± 0.2
T6_500_GAL	37.2 ± 0.2	2.3 ± 0.3
T9_1000	25.9 ± 0.2	2.1 ± 0.4
T9_1000_GLU	30.7 ± 0.5	2.1 ± 0.6
T9_1000_GAL	35.3 ± 0.4	2.5 ± 0.4

† Resulting from the fitting of SAXS curves according to a *Lorentzian* contribution.

‡ Obtained from OM images according to Equation 2. The average values and the standard deviations resulting from of analysis of three particles *per* sample are reported.

The ability of both pristine and cross-linked micro-particles to absorb water was investigated by swelling the microparticles in an excess of water (see section 2.4.5) and evaluating the ratio between the diameter of a swelled microparticle and that of the same microparticle when dry. The results (reported in Table 3 and Figure S5) show that the hydration produces a strong increase of the volume in all the samples, on average by a factor of around 20 times. Most importantly, the swelling ability is retained also in cross-linked samples, confirming the considerations drawn from SAXS results. The

experiments were also conducted at 37 °C (only for the cross-linked samples, as pristine microparticles dissolve after few minutes at this temperature), showing no significant difference with respect to the behavior at room temperature. As introduced before, the stability of gelatin microparticles against dissolution is of crucial towards their application, especially at human body temperature. To assess this aspect, the dissolution of the samples in water at 37 ˚C was assessed as described in section 2.4.6. Pristine samples dissolve within few minutes, while cross-linking with GAL and GLU prolongs the stability over few hours and few days. Representative optical microscopy images of T9_1000, T9_1000_GAL and T9_1000_GLU at different times are shown in Figure 7 (corresponding micrographs for T3_500 and T6_500 samples are given in the Supplementary Material), showing that microparticles are swelled by water, but their stability is strongly enhanced over time scales relevant to food and biomedical applications, with the possibility to tune it by using different cross-linkers.

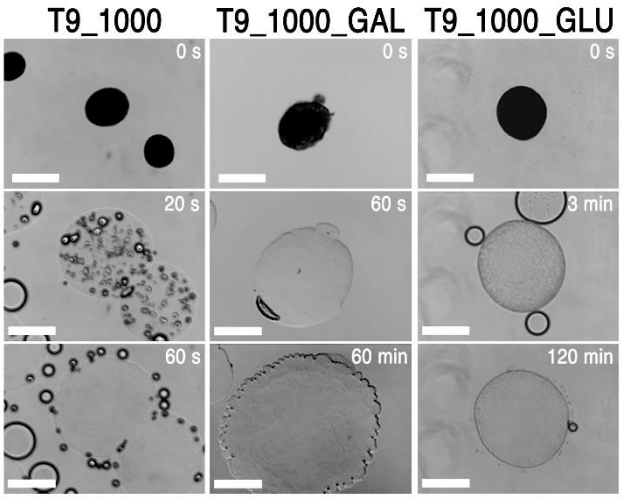

Figure 7. Optical microscopy micrographs of the dissolution process of samples T9_1000 (first column), T9_1000_GAL (second column) and T9_1000_GLU (third column). The time elapsed from the addition of water to dry microparticles is reported on each image (top right). The scale bar is 200 μm.

4. Conclusions

In summary, the results presented in this paper show that the double emulsion method is highly effective towards the preparation of gelatin porous microparticles with tunable shape, size and porosity. Oil droplets are first stabilized in a gelatin/water matrix with the aid of a non-ionic surfactant. The resulting emulsion is then dispersed in oil in the form of oil-in-water droplets using another non-ionic surfactant and the droplets are converted into porous microparticles. Combining multiple microscopy techniques, we thoroughly assessed the effect of the stirring speed and the

gelatin/surfactant ratio on the microparticles structural properties, including surface and inner porosities. The results allowed us to establish some general guidelines for the preparation of porous gelatin microparticles with tailored morphologies: *i.* lowering the gelatin/surfactant ratio takes to the formation of spherical particles; *ii.* increasing the gelatin/surfactant ratio produces wrinkled particles with irregular shapes; *iii.* the size of the particles and their polydispersity diminishes as the stirring speed is increased; *iv.* low stirring speeds and high gelatin/surfactant ratios lead to large pores. The preparation of porous gelatin microparticles has been previously reported in the literature (Lan et al., 2017; Li et al., 2020; Nilsson et al., 1986; Tao et al., 2003; Wang et al., 2012; Yamashita et al., 2009); nevertheless, to the best of our knowledge, the effect of the preparation protocol has not been addressed up to now with such a systematic approach. The possibility to tailor the size and the surface features of gelatin microparticles is of utmost importance to many applications, as well as enhancing their stability against dissolution, especially when the application takes place in aqueous environments at physiological temperature. To this aim, we successfully cross-linked the microparticles with two bifunctional molecules (namely, glutaraldehyde and glyceraldehyde), managing to extend the stability up to hours or days, depending on the cross-linker, without hindering the ability of microparticles to swell in water. This agrees with the typical nanoscale structure of gelatin being preserved upon cross-linking, as shown by the mesh size of the chains transient network measured by scattering experiments. The findings reported in this work provide fundamental insights towards the preparation of porous gelatin microparticles for highly relevant applications where tunable porosity and roughness of the substrate is crucial, *e.g.*, as drug delivery vehicles (Kaczmarek & Sionkowska, 2017) or as scaffolds for the adhesion and proliferation of anchorage-dependent cells (Huang et al., 2009).

Acknowledgements

CSGI (Consorzio Interuniversitario per lo Sviluppo dei Sistemi a Grande Interfase), Fondazione CR Firenze (project 2017.0720) and MIUR-Italy ("Progetto Dipartimenti di Eccellenza 2018–2022" allocated to Department of Chemistry "Ugo Schiff") are acknowledged for financial support.

This work benefited from the use of the SasView application, originally developed under NSF Award DMR-0520547. SasView also contains code developed funding from the EU Horizon 2020 programme under the SINE2020 project Grant No 654000.

References

Ahammed, S., Liu, F., Khin, M. N., Yokoyama, W. H., & Zhong, F. (2020). Improvement of the water resistance and ductility of gelatin film by zein. *Food Hydrocolloids*, *105*, 105804. https://doi.org/10.1016/j.foodhyd.2020.105804

Bancel, S., & Hu, W.-S. (1996). Confocal Laser Scanning Microscopy Examination of Cell Distribution in Macroporous Microcarriers. *Biotechnology Progress*, *12*(3), 398–402. https://doi.org/10.1021/bp960023a

Bello, A. B., Kim, D., Kim, D., Park, H., & Lee, S.-H. (2020). Engineering and Functionalization of Gelatin Biomaterials: From Cell Culture to Medical Applications. *Tissue Engineering Part B: Reviews*, *26*(2), 164–180. https://doi.org/10.1089/ten.teb.2019.0256

Bigi, A., Cojazzi, G., Panzavolta, S., Roveri, N., & Rubini, K. (2002). Stabilization of gelatin films by crosslinking with genipin. *Biomaterials*, *23*(24), 4827–4832.

Bigi, A., Cojazzi, G., Panzavolta, S., Rubini, K., & Roveri, N. (2001). Mechanical and thermal properties of gelatin films at different degrees of glutaraldehyde crosslinking. *Biomaterials*, *22*(8), 763–768. https://doi.org/10.1016/S0142-9612(00)00236-2

Campiglio, C. E., Contessi Negrini, N., Farè, S., & Draghi, L. (2019). Cross-Linking Strategies for Electrospun Gelatin Scaffolds. *Materials*, *12*(15), 2476. https://doi.org/10.3390/ma12152476

Chang, J.-Y., Lin, J.-H., Yao, C.-H., Chen, J.-H., Lai, T.-Y., & Chen, Y.-S. (2007). In vivo evaluation of a biodegradable EDC/NHS-cross-linked gelatin peripheral nerve guide conduit material. *Macromolecular Bioscience*, *7*(4), 500–507. https://doi.org/10.1002/mabi.200600257

Chang, M. C., & Tanaka, J. (2002). FT-IR study for hydroxyapatite/collagen nanocomposite cross-linked by glutaraldehyde. *Biomaterials*, *23*(24), 4811–4818. https://doi.org/10.1016/S0142-9612(02)00232-6

Choktaweesap, N., Arayanarakul, K., Aht-ong, D., Meechaisue, C., & Supaphol, P. (2007). Electrospun Gelatin Fibers: Effect of Solvent System on Morphology and Fiber Diameters. *Polymer Journal*, *39*(6), 622–631. https://doi.org/10.1295/polymj.PJ2006190

Devi, N., & Kakati, D. K. (2013). Smart porous microparticles based on gelatin/sodium alginate polyelectrolyte complex. *Journal of Food Engineering*, *117*(2), 193–204. https://doi.org/10.1016/j.jfoodeng.2013.02.018

Dias, A. D., Elicson, J. M., & Murphy, W. L. (2017). Microcarriers with Synthetic Hydrogel Surfaces for Stem Cell Expansion. *Advanced Healthcare Materials*, *6*(16), 1700072. https://doi.org/10.1002/adhm.201700072

Dias, J. R., Baptista-Silva, S., Oliveira, C. M. T. de, Sousa, A., Oliveira, A. L., Bártolo, P. J., & Granja, P. L. (2017). In situ crosslinked electrospun gelatin nanofibers for skin regeneration. *European Polymer Journal*, *95*, 161–173. https://doi.org/10.1016/j.eurpolymj.2017.08.015

Elzoghby, A. O. (2013). Gelatin-based nanoparticles as drug and gene delivery systems: Reviewing three decades of research. *Journal of Controlled Release*, *172*(3), 1075–1091. https://doi.org/10.1016/j.jconrel.2013.09.019

Esposito, E., Cortesi, R., & Nastruzzi, C. (1996). Gelatin microspheres: Influence of preparation parameters and thermal treatment on chemico-physical and biopharmaceutical properties. *Biomaterials*, *17*(20), 2009–2020. https://doi.org/10.1016/0142-9612(95)00325-8

Foox, M., & Zilberman, M. (2015). Drug delivery from gelatin-based systems. *Expert Opinion on Drug Delivery*, *12*(9), 1547–1563. https://doi.org/10.1517/17425247.2015.1037272

Gao, S., Yuan, Z., Guo, W., Chen, M., Liu, S., Xi, T., & Guo, Q. (2017). Comparison of glutaraldehyde and carbodiimides to crosslink tissue engineering scaffolds fabricated by decellularized porcine menisci. *Materials Science and Engineering: C*, *71*, 891–900. https://doi.org/10.1016/j.msec.2016.10.074

Garti, N., & Bisperink, C. (1998). Double emulsions: Progress and applications. *Current Opinion in Colloid & Interface Science*, *3*(6), 657–667. https://doi.org/10.1016/S1359-0294(98)80096-4

Gelli, R., Del Buffa, S., Tempesti, P., Bonini, M., Ridi, F., & Baglioni, P. (2018). Enhanced formation of hydroxyapatites in gelatin/imogolite macroporous hydrogels. *Journal of Colloid and Interface Science*, *511*(Supplement C), 145–154. https://doi.org/10.1016/j.jcis.2017.09.094

Ghosh Dastidar, D., Saha, S., & Chowdhury, M. (2018). Porous microspheres: Synthesis, characterisation and applications in pharmaceutical & medical fields. *International Journal of Pharmaceutics*, *548*(1), 34–48. https://doi.org/10.1016/j.ijpharm.2018.06.015

Han, B., Jaurequi, J., Tang, B. W., & Nimni, M. E. (2003). Proanthocyanidin: A natural crosslinking reagent for stabilizing collagen matrices. *Journal of Biomedical Materials Research. Part A*, *65*(1), 118–124. https://doi.org/10.1002/jbm.a.10460

Harris, P., Normand, V., & Norton, I. T. (2003). Gelatin. In *Encyclopedia of Food Sciences and Nutrition* (pp. 2865–2871). Elsevier. https://doi.org/10.1016/B0-12-227055-X/00551-4

Haug, I. J., & Draget, K. I. (2011). Gelatin. In *Handbook of Food Proteins* (pp. 92–115). Elsevier. https://doi.org/10.1533/9780857093639.92

Huang, S., Wang, Y., Liang, T., Jin, F., Liu, S., & Jin, Y. (2009). Fabrication and characterization of a novel microparticle with gyrus-patterned surface and growth factor delivery for cartilage tissue engineering. *Materials Science and Engineering: C*, *29*(4), 1351–1356. https://doi.org/10.1016/j.msec.2008.10.036

Huss, F. R. M., Junker, J. P. E., Johnson, H., & Kratz, G. (2007). Macroporous gelatine spheres as culture substrate, transplantation vehicle, and biodegradable scaffold for guided regeneration of soft tissues. In vivo study in nude mice. *Journal of Plastic, Reconstructive & Aesthetic Surgery*, *60*(5), 543–555. https://doi.org/10.1016/j.bjps.2005.10.031

Huss, F. R. M., Nyman, E., Bolin, J. S. C., & Kratz, G. (2010). Use of macroporous gelatine spheres as a biodegradable scaffold for guided tissue regeneration of healthy dermis in humans: An in vivo study. *Journal of Plastic, Reconstructive & Aesthetic Surgery*, *63*(5), 848–857. https://doi.org/10.1016/j.bjps.2009.01.068

Imparato, G., Urciuolo, F., Casale, C., & Netti, P. A. (2013). The role of microscaffold properties in controlling the collagen assembly in 3D dermis equivalent using modular tissue engineering. *Biomaterials*, *34*(32), 7851–7861. https://doi.org/10.1016/j.biomaterials.2013.06.062

JL Gornall, E. T. (2008). Helix-coil transition of gelatin: Helical morphology and stability. *Soft Matter*, *4*(3), 544–549. https://doi.org/10.1039/B713075A

Kaczmarek, B., & Sionkowska, A. (2017). Drug Release from Porous Matrixes based on Natural Polymers. *Current Pharmaceutical Biotechnology*, *18*(9). https://doi.org/10.2174/1389201018666171103141347

Karimian S.A., M., Mashayekhan, S., & Baniasadi, H. (2016). Fabrication of porous gelatin-chitosan microcarriers and modeling of process parameters via the RSM method. *International Journal of Biological Macromolecules*, *88*, 288–295. https://doi.org/10.1016/j.ijbiomac.2016.03.061

Kim, J., Yaszemski, M. J., & Lu, L. (2009). Three-Dimensional Porous Biodegradable Polymeric Scaffolds Fabricated with Biodegradable Hydrogel Porogens. *Tissue Engineering. Part C, Methods*, *15*(4), 583–594. https://doi.org/10.1089/ten.tec.2008.0642

Kuijpers, A. J., Engbers, G. H., Krijgsveld, J., Zaat, S. A., Dankert, J., & Feijen, J. (2000). Cross-linking and characterisation of gelatin matrices for biomedical applications. *Journal of Biomaterials Science. Polymer Edition*, *11*(3), 225–243. https://doi.org/10.1163/156856200743670

Lan, L., Tian, F.-R., ZhuGe, D.-L., ZhuGe, Q.-C., Shen, B.-X., Jin, B.-H., Huang, J.-P., Wu, M.-Z., Fan, L.-X., Zhao, Y.-Z., & Xu, H.-L. (2017). Implantable porous gelatin microspheres

sustained release of bFGF and improved its neuroprotective effect on rats after spinal cord injury. *PLOS ONE*, *12*(3), e0173814. https://doi.org/10.1371/journal.pone.0173814

Lengyel, M., Kállai-Szabó, N., Antal, V., Laki, A. J., & Antal, I. (2019). Microparticles, Microspheres, and Microcapsules for Advanced Drug Delivery. *Scientia Pharmaceutica*, *87*(3), 20. https://doi.org/10.3390/scipharm87030020

Li, L., Du, Y., Yin, Z., Li, L., Peng, H., Zheng, H., Yang, A., Li, H., & Lv, G. (2020). Preparation and the hemostatic property study of porous gelatin microspheres both in vitro and in vivo. *Colloids and Surfaces B: Biointerfaces*, *187*, 110641. https://doi.org/10.1016/j.colsurfb.2019.110641

Liang, H.-C., Chang, W.-H., Liang, H.-F., Lee, M.-H., & Sung, H.-W. (2004). Crosslinking structures of gelatin hydrogels crosslinked with genipin or a water-soluble carbodiimide. *Journal of Applied Polymer Science*, *91*(6), 4017–4026. https://doi.org/10.1002/app.13563

Lien, S.-M., Li, W.-T., & Huang, T.-J. (2008). Genipin-crosslinked gelatin scaffolds for articular cartilage tissue engineering with a novel crosslinking method. *Materials Science and Engineering: C*, *28*(1), 36–43. https://doi.org/10.1016/j.msec.2006.12.015

Lönnqvist, S., Rakar, J., Briheim, K., & Kratz, G. (2015). Biodegradable Gelatin Microcarriers Facilitate Re-Epithelialization of Human Cutaneous Wounds—An In Vitro Study in Human Skin. *PLOS ONE, 10*(6), e0128093. https://doi.org/10.1371/journal.pone.0128093

Ma, G., & Su, Z.-G. (2013). *Microspheres and Microcapsules in Biotechnology: Design, Preparation and Applications*. CRC Press.

Moll, F., Rosenkranz, H., & Himmelmann, W. (1974). The Structure of Gelatin Crosslinked with Formaldehyde. *The Journal of Photographic Science*, *22*(6), 255–261. https://doi.org/10.1080/00223638.1974.11737791

Nagura, M., Yokota, H., Ikeura, M., Gotoh, Y., & Ohkoshi, Y. (2002). Structures and Physical Properties of Cross-Linked Gelatin Fibers. *Polymer Journal*, *34*(10), 761–766. https://doi.org/10.1295/polymj.34.761

Ng, Y.-C., Berry, J. M., & Butler, M. (1996). Optimization of physical parameters for cell attachment and growth on macroporous microcarriers. *Biotechnology and Bioengineering*, *50*(6), 627–635. https://doi.org/10.1002/(SICI)1097-0290(19960620)50:6<627::AID-BIT3>3.0.CO;2-M

Nguyen, A. H., McKinney, J., Miller, T., Bongiorno, T., & McDevitt, T. C. (2015). Gelatin methacrylate microspheres for controlled growth factor release. *Acta Biomaterialia*, *13*, 101–110. https://doi.org/10.1016/j.actbio.2014.11.028

Nikolai, T. J., & Hu, W.-S. (1992). Cultivation of mammalian cells on macroporous microcarriers. *Enzyme and Microbial Technology*, *14*(3), 203–208. https://doi.org/10.1016/0141-0229(92)90067-X

Nilsson, K., Buzsaky, F., & Mosbach, K. (1986). Growth of Anchorage–Dependent Cells on Macroporous Microcarriers. *Bio/Technology*, *4*(11), 989–990. https://doi.org/10.1038/nbt1186-989

Pezron, I., Djabourov, M., & Leblond, J. (1991). Conformation of gelatin chains in aqueous solutions: 1. A light and small-angle neutron scattering study. *Polymer*, *32*(17), 3201–3210. https://doi.org/10.1016/0032-3861(91)90143-7

Phromsopha, T., & Baimark, Y. (2014). Preparation of Starch/Gelatin Blend Microparticles by a Water-in-Oil Emulsion Method for Controlled Release Drug Delivery. *International Journal of Biomaterials*, *ID 829490*, e829490. https://doi.org/10.1155/2014/829490

Rao, Y. (2007). Gelatin–clay nanocomposites of improved properties. *Polymer*, *48*(18), 5369–5375. https://doi.org/10.1016/j.polymer.2007.06.068

Ratanavaraporn, J., Rangkupan, R., Jeeratawatchai, H., Kanokpanont, S., & Damrongsakkul, S. (2010). Influences of physical and chemical crosslinking techniques on electrospun type A and B gelatin fiber mats. *International Journal of Biological Macromolecules*, *47*(4), 431–438. https://doi.org/10.1016/j.ijbiomac.2010.06.008

Rodrigues, M. E. (2013). Evaluation of Macroporous and Microporous Carriers for CHO-K1 Cell Growth and Monoclonal Antibody Production. *Journal of Microbiology and Biotechnology*, *23*(9), 1308–1321. https://doi.org/10.4014/jmb.1304.04011

Santoro, M., Tatara, A. M., & Mikos, A. G. (2014). Gelatin carriers for drug and cell delivery in tissue engineering. *Journal of Controlled Release*, *190*, 210–218. https://doi.org/10.1016/j.jconrel.2014.04.014

Schneider, C. A., Rasband, W. S., & Eliceiri, K. W. (2012). NIH Image to ImageJ: 25 years of image analysis. *Nature Methods*, *9*(7), 671–675. https://doi.org/10.1038/nmeth.2089

Shiragami, N., Honda, H., & Unno, H. (1993). Anchorage-dependent animal cell culture by using a porous microcarrier. *Bioprocess Engineering*, *8*(5), 295–299. https://doi.org/10.1007/BF00369844

Sisson, K., Zhang, C., Farach-Carson, M. C., Chase, D. B., & Rabolt, J. F. (2009). Evaluation of Cross-Linking Methods for Electrospun Gelatin on Cell Growth and Viability. *Biomacromolecules*, *10*(7), 1675–1680. https://doi.org/10.1021/bm900036s

Su, K., & Wang, C. (2015). Recent advances in the use of gelatin in biomedical research. *Biotechnology Letters*, *37*(11), 2139–2145. https://doi.org/10.1007/s10529-015-1907-0

Sulaiman, S. B., Idrus, R. B. H., & Hwei, N. M. (2020). Gelatin Microsphere for Cartilage Tissue Engineering: Current and Future Strategies. *Polymers*, *12*(10), 2404. https://doi.org/10.3390/polym12102404

Tao, X., Shaolin, L., & Yaoting, Y. (2003). Preparation and culture of hepatocyte on gelatin microcarriers. *Journal of Biomedical Materials Research*, *65A*(2), 306–310. https://doi.org/10.1002/jbm.a.10277

Tatini, D., Tempesti, P., Ridi, F., Fratini, E., Bonini, M., & Baglioni, P. (2015). Pluronic/gelatin composites for controlled release of actives. *Colloids and Surfaces B: Biointerfaces*, *135*, 400–407. https://doi.org/10.1016/j.colsurfb.2015.08.002

Vandelli, M. A., Rivasi, F., Guerra, P., Forni, F., & Arletti, R. (2001). Gelatin microspheres crosslinked with d,l-glyceraldehyde as a potential drug delivery system: Preparation, characterisation, in vitro and in vivo studies. *International Journal of Pharmaceutics*, *215*(1), 175–184. https://doi.org/10.1016/S0378-5173(00)00681-5

Vargas, G., Acevedo, J. L., López, J., & Romero, J. (2008). Study of cross-linking of gelatin by ethylene glycol diglycidyl ether. *Materials Letters*, *62*(21–22), 3656–3658. https://doi.org/10.1016/j.matlet.2008.04.020

Vesperinas, A., Eastoe, J., Wyatt, P., Grillo, I., & Heenan, R. K. (2006). Photosensitive gelatin. *Chemical Communications*, *42*, 4407. https://doi.org/10.1039/b609267e

Wang, A., Cui, Y., Li, J., & Hest, J. C. M. van. (2012). Fabrication of Gelatin Microgels by a "Cast" Strategy for Controlled Drug Release. *Advanced Functional Materials*, *22*(13), 2673–2681. https://doi.org/10.1002/adfm.201102907

Wu, X., Liu, Y., Li, X., Wen, P., Zhang, Y., Long, Y., Wang, X., Guo, Y., Xing, F., & Gao, J. (2010). Preparation of aligned porous gelatin scaffolds by unidirectional freeze-drying method. *Acta Biomaterialia*, *6*(3), 1167–1177. https://doi.org/10.1016/j.actbio.2009.08.041

Xia, P., Wang, S., Qi, Z., Zhang, W., & Sun, Y. (2019). BMP-2-releasing gelatin microspheres/PLGA scaffolds for bone repairment of X-ray-radiated rabbit radius defects. *Artificial Cells, Nanomedicine, and Biotechnology*, *47*(1), 1662–1673. https://doi.org/10.1080/21691401.2019.1594852

Yamashita, N., Izumikawa, S., Takagi, A., Arakawa, H., Wakasawa, T., & Maruyama, A. (2009). Preparation and characterization of gelatin sponge millispheres from air-in-water-in-oil-type emulsions. *Journal of Materials Science: Materials in Medicine*, *20*(6), 1299–1305. https://doi.org/10.1007/s10856-008-3681-1

Yuan, L., Li, X., Ge, L., Jia, X., Lei, J., Mu, C., & Li, D. (2019). Emulsion Template Method for the Fabrication of Gelatin-Based Scaffold with a Controllable Pore Structure. *ACS Applied Materials & Interfaces*, *11*(1), 269–277. https://doi.org/10.1021/acsami.8b17555

Zhang, S., Huang, Y., Yang, X., Mei, F., Ma, Q., Chen, G., Ryu, S., & Deng, X. (2009). Gelatin nanofibrous membrane fabricated by electrospinning of aqueous gelatin solution for guided tissue regeneration. *Journal of Biomedical Materials Research Part A, 90A*(3), 671–679. https://doi.org/10.1002/jbm.a.32136